

## Research Article

# A New Technique for Integrating MEMS-Based Low-Cost IMU and GPS in Vehicular Navigation

Neda Navidi,<sup>1</sup> René Jr. Landry,<sup>1</sup> Jianhua Cheng,<sup>2</sup> and Denis Gingras<sup>3</sup>

<sup>1</sup>LASSEN Laboratory, École de Technologie Supérieure, 1100 Notre-Dame Street West, Montreal, QC, Canada H3C 1K3

<sup>2</sup>Marine Navigation Research Institute, College of Automation, Harbin Engineering University, Harbin 150001, China

<sup>3</sup>LIV Laboratory, Electrical and Computer Engineering Department, Université de Sherbrooke, Sherbrooke, QC, Canada J1K 2R1

Correspondence should be addressed to Neda Navidi; [neda.nav3@gmail.com](mailto:neda.nav3@gmail.com)

Received 20 November 2015; Revised 4 April 2016; Accepted 28 April 2016

Academic Editor: Maan E. El Najjar

Copyright © 2016 Neda Navidi et al. This is an open access article distributed under the Creative Commons Attribution License, which permits unrestricted use, distribution, and reproduction in any medium, provided the original work is properly cited.

In providing acceptable navigational solutions, Location-Based Services (LBS) in land navigation rely mostly on integration of Global Positioning System (GPS) and Inertial Navigation System (INS) measurements for accuracy and robustness. The GPS/INS integrated system can provide better land-navigation solutions than the ones any standalone system can provide. Low-cost Inertial Measurement Units (IMUs), based on Microelectromechanical Systems (MEMS) technology, revolutionized the land-navigation system by virtue of their low-cost miniaturization and widespread availability. However, their accuracy is strongly affected by their inherent systematic and stochastic errors, which depend mainly on environmental conditions. The environmental noise and nonlinearities prevent obtaining optimal localization estimates in Land Vehicular Navigation (LVN) while using traditional Kalman Filters (KF). The main goal of this paper is to effectively eliminate stochastic errors of MEMS-based IMUs. The proposed solution is divided into two main components: (1) improving noise cancellation, using advanced stochastic error models in MEMS-based IMUs based on combined Autoregressive Processes (ARP) and first-order Gauss-Markov Process (1GMP), and (2) modeling the low-cost GPS/INS integration, using a hybrid Fuzzy Inference System (FIS) and Second-Order Extended Kalman Filter (SOEKF). The results obtained show that the proposed methods perform better than the traditional techniques do in different stochastic and dynamic situations.

## 1. Introduction

Steadily increasing economical and environmental constraints as well as stringent safety requirements have triggered the development and widespread use of low-cost Land Vehicular Navigation (LVN) systems over the last decade. LVNs have many applications: nonsafety applications, such as fleet management and traffic optimization, or active safety applications, such as Collision Mitigation Braking Systems (CMBS) and lane keeping systems. LVNs can also be used for protecting vehicles from theft in vehicle tracking systems or for reducing the greenhouse gas emissions in environmental monitoring systems. Besides, they can also be used in autonomous car navigation systems and emergency assistance services. Furthermore, the need for recognizing driver's behavior in many applications requires low-cost and reliable

estimation of vehicular position and attitude. Clearly, universal use of LVN in road transportation demands lower cost, widespread availability, and ever improving performance [1].

Advanced commercial Location-Based Services (LBS) must be able to solve difficult positioning problems, especially those in indoor-parking, urban canyons, or dense foliage situations, by providing acceptable customer support, whenever the GPS signal is lost. One issue that is recently investigated in positioning-based systems relies on multi-Global Navigation Satellite Systems (GNSS) environment which is realized due to the effective usage of the global constellation of GLONASS, satellites of Galileo, and Chinese BeiDou Navigation Satellite System (BDS). Multi-GNSS environment offers several advantages over a standalone GPS. Indeed, multi-GNSS environment may increase the availability of navigation satellites where the received GPS signals are less

than 4 satellites in urban canyons. Moreover, it can improve the accuracy of positioning, especially when the navigation system considers the horizontal positioning accuracy [2].

However, multi-GNSS-based techniques may increase the intersystem interference, particularly when multi-GNSS environments broadcast navigation signals in overlapped frequency bands. Moreover, these techniques impose higher levels of complexity, because the analog-part of the receiver should deal with multiple-system, multiple frequencies and considerable bandwidths [3]. Finally, the mentioned developed techniques consist in postprocessing techniques that require laborious manipulations and calculations, which may not be suitable for real-time commercial applications. A modern approach to solve the current positioning problems is to integrate the GPS signals with Low-cost Inertial Measurement Units (IMUs) data. IMUs can estimate the position and the attitude of the vehicle by employing an Inertial Navigation System (INS) mechanization process (accelerometers and gyroscopes), which is an integration of linear accelerations and angular rates. However, MEMS-based low-cost IMUs perform accurately just for a limited time as their positioning and attitudinal errors increase steadily with time.

MEMS-based IMUs are classified based on their mass position recognition, their operation mode, and their fabrication procedure. Piezoresistive, Capacitive, Piezoelectric, and Resonant element sensors are different types of MEMS sensors which are placed in the classification of mass position recognition [4]. These types of sensors transform the physical work caused by variation of movement into an electrical signal. Piezoresistive and Piezoelectric sensors are widely used in MEMS-based IMUs because of their simplicity, cost-effectiveness, and wide dynamic range. However, they suffer from low precision and high sensitivity to temperature [4]. Performance characteristics of MEMS-based sensors include bandwidth, noise floor, misalignment, drift, linearity, dynamic range, and power consumption. Thus, the MEMS-based inertial sensor errors are generally composed of stochastic errors which have an undesirable impact on the quality of the navigation solution [5].

The first part of the proposed methodology consists of augmenting the navigation solution with 1st-order Gauss-Markov Process (IGMP) for dynamically estimating and compensating the stochastic errors of MEMS-based low-cost IMUs. Two different identification methods were exploited in this study to identify the IGMP parameters. The first one is a traditional method based on the analysis of Autocorrelation Function (ACF) and the second one is based on analysis of 1st-order Autoregressive Process (ARP) model. ACF does not fully match the random error characteristics of low-cost MEMS-based IMUs. What mainly causes this mismatch is the high nonlinearity of the low-cost inertial sensor errors leading to higher order GMPs (i.e., 2nd- or 3rd-order GMPs) distributions instead of IGMP [6]. Thus, there is a need for the development of better model-based methods to accurately estimate the distribution of the IGMP low-cost inertial sensor errors. This study proposes using combined IGMP-ARP method as an alternative candidate to identify the IGMP's parameters distribution in the low-cost inertial sensors. To estimate the ARP's coefficients,

three different algorithms were considered and implemented, namely, the Yule-Walker (YW) method, the Burg method, and the modified-covariance method [7].

As these static errors have both high frequency (HF) term and low frequency (LF) term, decreasing both of them is needed in order to develop the accuracy of the low-cost inertial sensors. Wavelet Denoising Techniques (WDTs) have been utilized in similar research studies, due to their significant role in removing the HF noises [8]. So, it is presented a mixture of the WDT (with different levels) and IGMP to evaluate the accuracy improvement of the low-cost inertial sensors when these methods are blended together.

Traditionally, GPS/INS integration is carried out by using Kalman Filter (KF) techniques. This approach has been validated in many studies, where high-end IMUs were used [9]. However, recent studies report several shortcomings in KF-based INS/GPS integration, when using low-cost MEMS-based inertial sensors [6]. Dynamic models that define the navigation problem are originally nonlinear [10], but, to allow the use of simple linear filters such as the KF, these models are generally linearized under a small error assumption. With the assumption made by the KF that the system is characterized by a linear model, driven by white Gaussian noise, it is not possible to describe the nonlinear error dynamics of MEMS-based INS [11].

The conventional 1st-order EKF is used extensively for integration of high-end INS and GPS data, which can achieve a suboptimal estimation of Minimum Mean Square Error (MMSE) of the vehicle state vector [12]. 1st-order Extended Kalman Filter (EKF) is based on the assumption that the higher order terms (2nd-order and up) of a Taylor series expansion are small enough to be ignored. This condition may hold for high-end navigation systems where the errors are kept small and bounded, but not for highly nonlinear systems, such as MEMS-based INS. In addition, to provide an acceptable position and attitude estimates, the 1st-order EKF requires proper nonlinear models of vehicle dynamics and measurement sensors. The first-order linearization, especially in the presence of highly nonlinear dynamics, often leads to divergence of the state covariance matrix [11]. Thus, using such assumption for a low-cost navigation system may result in unstable solution, as demonstrated by several previously published results [13].

Several research groups investigated the possibility of using sampling techniques to cope with highly non-Gaussian multimodal error distributions in GPS/INS integration and thus avoiding linearization of the dynamic models [13]. Unscented Kalman Filter (UKF) and Particle Filter (PF) are two such alternative methods that can provide better performance than does classical KF or EKF, but at high computational costs [11, 14]. Some authors assert that the limitations of the sampling and the Kalman-based techniques can be overcome by using Artificial Intelligence (AI) [15]. The integration of AI algorithms with next generation embedded navigation systems is made possible with the technological advancement in computer technologies. In the last decade, various neural networks (NN) and Fuzzy Inference Systems- (FIS-) based integration scheme were introduced [16–18]. AI algorithms require a training phase, which is realized

during GPS signal availability using a learning algorithm. However, AI-based GPS/INS integration schemes suffer from two main drawbacks: these methods generally require long training time that greatly limits their utilization in a real-time commercial application; moreover, they highly depend on the consistency of the training data and show limited success if the error dynamics do not stay the same between their training and prediction stages [11].

The second part of the proposed approach is to combine both linearized navigation filters and AI techniques into an intelligent cognitive navigator. SOEKF as the linearized navigation filter helps in reducing the linearization error during the filtering process and FIS-based approach as an AI technique, predicting the error states of the SOEKF based on a Covariance Matching Estimation Technique (COMET). In fact, the dynamic characteristics of vehicle motion in body frame and the navigation frame form based on the SOEKF process. The FIS can be exploited to increase the accuracy and the robustness of the SOEKF and to prevent its divergence in the tuning phase of SOEKF. The performances of the proposed methods were evaluated by a road test, using Matlab. The results show that the proposed method is effective in reducing the root mean square error (RMSE) of position by 45% compared with the SOEKF.

The remainder of the paper is organized as follows: Section 2 describes the main methods of this study. Section 3 deals with the proposed methods and the contributions of this paper for GPS/INS integration and the noise modeling. The method employed here for the GPS/INS integration is based on the proposed hybrid FIS-SOEKF model. Additionally, the proposed noise modeling of low-cost inertial sensor utilizes the combined IGMP-ARP. Section 4 deals with the road test and the detailed analysis of experimental data, followed by a discussion on the performance obtained. Finally, Section 5 concludes this paper by summarizing the results achieved and by offering suggestions for future work to improve the proposed methods.

## 2. Background

This section presents details on background of techniques and ideas used in this study. More specifically, two main topics will be studied in this section: Second-Order Extended Kalman Filter (SOEKF) as a data-fusion technique for automotive navigation and stochastic error modeling technique in Inertial Navigation Systems.

**2.1. Second-Order Extended Kalman Filter (SOEKF).** Linear state estimators have been widely used in the early literature for guidance, navigation, and control of various types of vehicles, including aircraft, space shuttles, ships, submarines, and automotive land vehicles [9]. As mentioned in Introduction, in order to perform optimal estimation using the classical Kalman Filter-based technique on the nonlinear and stochastic INS dynamic model, the model must be linearized around assumptions. First-order and second-order Extended Kalman Filter (EKF) are two Kalman Filter-based techniques which linearized based on the assumption of first and second orders of a Taylor series expansion.

In this study, SOEKF was addressed for proposed data-fusion of low-cost INS and GPS aided with FIS. Thus, a summary of SOEKF performance is presented in this section. The SOEKF is an estimator method, which can solve the problem of estimating the state of a controlled process. The model of SOEKF is

$$\begin{aligned}\bar{\bar{x}}_k &= f(x_{k-1}, k-1) + q_{k-1}, \\ \bar{\bar{y}}_k &= h(x_k, k) + r_k,\end{aligned}\quad (1)$$

where  $\bar{\bar{x}}_k \in \mathbb{R}^m$  is the state,  $\bar{\bar{y}}_k \in \mathbb{R}^m$  is the measurement,  $q_{k-1} \sim N(0, Q_k)$  is the process noise,  $r_k \sim N(0, R_k)$  is measurement noise, and  $f$  and  $h$  are the dynamic and measurement model functions. The prediction and correction steps of SOEKF are described by [19–21]

$$\begin{aligned}\hat{x}_k^- &= f(x_{k-1}, k-1) + \frac{1}{2} \sum_i e_i \text{tr} \{F_{xx}^{(i)}(x_{k-1}, k-1) \\ &\cdot P_{k-1}\}, \\ P_k^- &= F_x(x_{k-1}, k-1) P_{k-1} F_x^T(\hat{x}_{k-1}, k-1) + \frac{1}{2} \sum_i e_i \\ &\cdot e_i^T \text{tr} \{F_{xx}^{(i)}(x_{k-1}, k-1) P_{k-1} F_{xx}^{(i')}(\hat{x}_{k-1}, k-1) P_{k-1}\} \\ &+ \eta_k,\end{aligned}\quad (2)$$

where  $\hat{x}_k^-$  and  $P_k^-$  are, respectively, the time-propagated state estimates and covariance  $F_k$  and  $H_k$  are the state transition and the design matrices;  $x_k$  is the error state vector and  $z_k$  the measurement vector:

$$v_k = z_k - h(x_k^-, k) + \frac{1}{2} \sum_i e_i \text{tr} \{H_{xx}^{(i)}(x_k, k) P_k\}, \quad (3)$$

$$\begin{aligned}\text{COV}_k &= H_x(x_k^-, k) P_k^- H_x^T(x_k^-, k) \\ &+ \frac{1}{2} \sum_{i,i'} e_i e_{i'}^T \text{tr} \{H_{xx}^{(i)}(x_k^-, k) P_k^- H_{xx}^{(i')}(\hat{x}_k^-, k) P_k\} \\ &+ \mu_k,\end{aligned}\quad (4)$$

$$K_k = P_k^- H_x^T(x_k^-, k) + \text{COV}_k^{-1}, \quad (5)$$

$$x_k = x_k^- + K_k v_k, \quad (6)$$

$$P_k = P_k^- - K_k S_k K_k^T, \quad (7)$$

where  $F_x(x, k-1)$  and  $H_x(x, k)$  are Jacobian matrices of  $f_i$  and  $h_i$  which are expressed by

$$\begin{aligned}[F_x(x, k-1)]_{i,i'} &= \frac{\partial f_i(x, k-1)}{\partial x_{i'}}, \\ [H_x(x, k)]_{i,i'} &= \frac{\partial h_i(x, k)}{\partial x_{i'}},\end{aligned}\quad (8)$$

$F_{xx}^{(i)}(x, k-1)$  and  $H_{xx}^{(i)}(x, k)$  are the Hessian matrices of  $f_i$  and  $h_i$  which are defined by

$$\begin{aligned} [F_{xx}^{(i)}(x, k-1)]_{i,i'} &= \frac{\partial^2 f_i(x, k-1)}{\partial x_i \partial x_{i'}}, \\ [H_{xx}^{(i)}(x, k)]_{i,i'} &= \frac{\partial^2 h_i(x, k)}{\partial x_i \partial x_{i'}}, \end{aligned} \quad (9)$$

and  $e_i$  is the unit vector in direction of the coordinate axis  $i$ .

**2.2. Stochastic Error Modeling Technique in Inertial Navigation Systems.** Techniques developed for the correction of inertial sensor errors can generally be divided into two categories that are (1) deterministic error calibration procedures and (2) stochastic error estimation models. Only the stochastic error estimation models are considered in this work.

In general, stochastic errors can be separated into two categories, that is, white noise and colored (or correlated) noise. White noise is a random process characterized by an Autocorrelation Function (ACF) of the form of a Dirac. On the other hand, colored noise may exhibit different ACFs depending on the nature of the noise (pink, red, grey, etc.).

White noise can generally be mitigated using adequate low-pass filter or Wavelet Denoising Technique (WDT) while colored noise must be precisely modeled in order to be estimated and compensated. Traditionally, colored noise of IMUs is modeled as a first-order Gauss-Markov Process (IGMP) with an exponentially decaying ACF. This section presents details on stochastic processes to model the colored noise as well as Wavelet Denoising Technique (WDT) to eliminate the white noise in IMUs.

**2.2.1. Stochastic Processes.** The most important errors to consider are stochastic errors since these errors, if not dealt with, will have a significant negative impact on the accuracy of vehicular tracking output [5]. Several research groups started investigating the possibility of using Mont-Carlo simulation technique for modeling the stochastic errors of MEMS devices due to multicomponent character of the sensors. However, it increases the number of degrees of freedom in the dynamic model [22]. So the alternative methods like generalized stochastic perturbation technique, Stochastic Finite Element Method (SFEM), and Second-Order Second Moment (SOSM) approach are considered in [23–25].

Although there are several stochastic processes, this section addresses only those that were considered for this study, namely, first-order Gauss-Markov Process (IGMP) and Autoregressive Processes (ARP). The relation between these two stochastic processes and proposed stochastic error modeling will be detailed in Section 3.1.

**First-Order Gauss-Markov Process (IGMP).** Traditionally, the noises of IMUs are modeled as 1st-order Gauss-Markov Process (IGMP) [8, 26–28]. The continuous-time and the discrete-time models of GMP can be given, respectively, by (10) and (11). Consider

$$\dot{A}(t) = -\frac{A(t)}{T_c} + w(t), \quad (10)$$

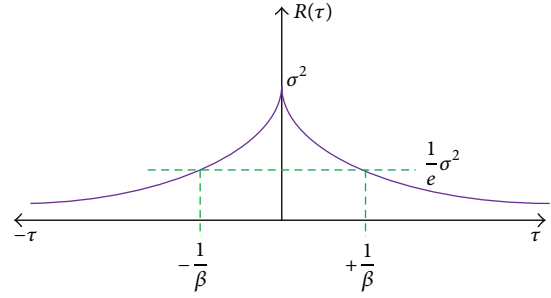


FIGURE 1: Autocorrelation Function (ACF) for IGMP.

$$A_{k+1} = e^{-\Delta t/T_c} \cdot A_k + w(n), \quad (11)$$

where  $A_k$  and  $w(n)$  are the IGMP and the white noise (WN) and  $\Delta t$  and  $T_c$  are the sampling and the correlation times, respectively. The noise covariance can be expressed by

$$\sigma_{wk}^2 = \sigma_{xk}^2 (1 - e^{-2\Delta t/T_c}). \quad (12)$$

Classically, IGMP's parameters can be estimated by Autocorrelation Function (ACF). Several studies investigated the use of ACF in analyzing the stochastic error of the inertial sensors and also to acquire IGMP's parameters. It can be modeled with an exponentially decaying ACF, as shown in Figure 1. The essential parameters required to model this process are  $\sigma^2$  and  $\beta$ , which are given by

$$R(\tau) = \sigma^2 e^{\beta|\tau|}, \quad \beta = \frac{1}{T_c}, \quad (13)$$

where  $\sigma^2$ ,  $\tau$ , and  $\beta$  are the noise covariance, the time lag, and the reciprocal of the process correlation time, respectively. As shown in Figure 1, this process limits the uncertainty of the signal, and this forms the distinctive feature of this process. And, so,  $R(\tau)$ , at any correlation time, is less than or equal to  $R(0)$ . However, the accuracy of ACF results depends on the length of the recorded data.

**Autoregressive Processes (ARP).** ACF might be matched to the higher order of GM, instead of the 1st-order one, for MEMS inertial sensors, as stated by many workers [29]. Thus, the other method to model the errors, which is presented in [29], is Autoregressive Processes (ARP). ARP is one type of Autoregressive Moving Average (ARMA) process, which is produced by the combination of past values and is expressed by

$$A_k = -\sum_{n=1}^b \alpha_n \cdot A_{k-n} + \beta_0 \omega_k, \quad (14)$$

where  $A_k$ ,  $b$ ,  $\alpha_n$ ,  $\beta_0$ , and  $\omega_k$  are the ARP output, order of process, model parameters, standard deviation, and white noise, respectively. Given the value of  $b$ , minimizing the root mean square error (RMSE) between the original signal and the signal estimated by ARP can help us to identify the ARP's coefficients. This error is presented by

$$\epsilon_k = \sum_k \left[ A_k + \sum_{n=1}^b \alpha_n A_{k-n} \right]^2. \quad (15)$$



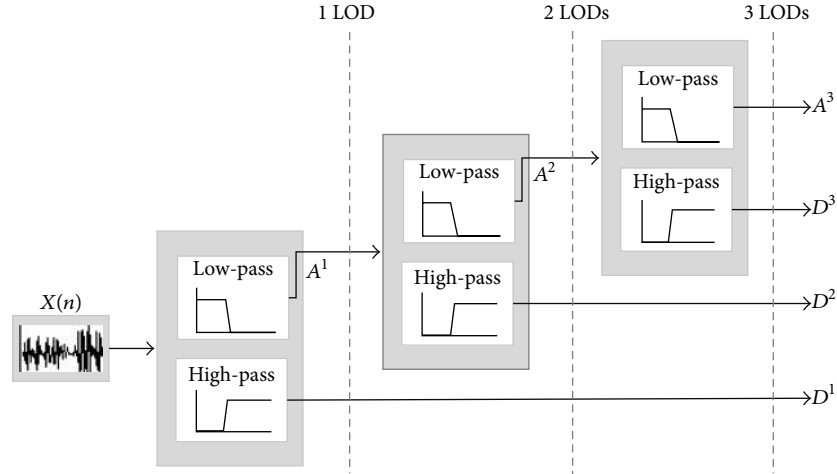


FIGURE 2: Application of Wavelet Denoising Technique (WDT) with different Levels of Decomposition (LODs).

There are several identification algorithms to estimate the ARP' coefficients. For this study, three methods, namely, Yule-Walker (YW), Burge's, and modified-covariance (MCOV) algorithms, will be considered for implementation. The method that gives the minimum RMSE will be the best one to estimate the ARP's coefficients. So, an investigation of the best method to estimate the ARP' coefficients is considered in this study.

**2.2.2. Wavelet Denoising Technique (WDT).** Wavelet Denoising Technique (WDT) is based on the wavelet filtering method, which can eliminate the stochastic error in the measurements of the inertial sensors at High Frequencies (HFs) without altering important information contained in the signal [30, 31]. A Multiresolution Analysis (MRA) algorithm was performed on the WDT, which can decompose a signal into different subbands with various time and frequency resolutions. Conceptually, in WDT, signal  $x(n)$  is filtered by one high-pass filter and one low-pass filter with downsampling by two ( $\downarrow 2$ ) in the continuous Levels of Decomposition (LODs), as shown in Figure 2.

The maximum amount of information about the original signal  $x(n)$  was contained in the approximation coefficients ( $A^k$ ) in each subband. Hence, the minority information of  $x(n)$  was contained in HF noise components, which were identified by detailed coefficients ( $D^k$ ). This technique can be combined with the different noise modeling process like IGMP and ARP, to investigate the stochastic error of inertial sensors. After applying the technique, the coefficients of IGMP were determined from the enduring noises. More related explanations are presented in Sections 3 and 4.

### 3. Proposed Methods

This paper proposes combining two independent and complementary solutions into a global integrated navigation system to provide stable low-cost ubiquitous automotive navigation in severe urban environments. The first proposed

solution consists of augmenting the navigation solution with combined IGMP-ARP for dynamically estimating and compensating the static errors of low-cost inertial. The second proposed solution is to combine both linearized navigation filters and AI techniques into an intelligent cognitive navigator. SOEKF as the linearized navigation filter helps in reducing the linearization error during the filtering process; and FIS-based approach as an AI technique helps in predicting the error states of the SOEKF. This section presents details on these two proposed solutions.

**3.1. Proposed Stochastic Error Modeling of Low-Cost IMU.** Autocorrelation Function (ACF), which is presented in Section 2, does not fully match the random error characteristics of low-cost MEMS-based IMUs. What mainly causes this mismatch is the high nonlinearity of the low-cost inertial sensor errors leading to other distributions instead of IGMP [6]. Thus, there is a need for the development of better model-based methods to accurately estimate the distribution of the IGMP low-cost inertial sensor errors. This study proposes using a new method, named "combined IGMP-ARP method," as an alternative candidate to identify the IGMP's parameters distribution in the low-cost inertial sensors. The fundamental concept of the model is IGMP. However, its  $\sigma^2$  and  $\beta$  are calculated by 1st-order ARP rather than by ACF. Substituting  $b = 1$  within (14) gives the first-order ARP as follows:

$$A_k = \alpha_1 \cdot A_{k-1} + \beta_0 \omega_k. \quad (16)$$

Combining (11) and (16), the value of  $\beta$  in IGMP can be related to  $\alpha_1$  in ARP as

$$\beta = -\ln \frac{\alpha_1}{\Delta t}. \quad (17)$$

In this study, we call this process "combined IGMP-ARP" model. The main advantage of the model is that the inaccurate ACF does not have a detrimental effect on the estimated

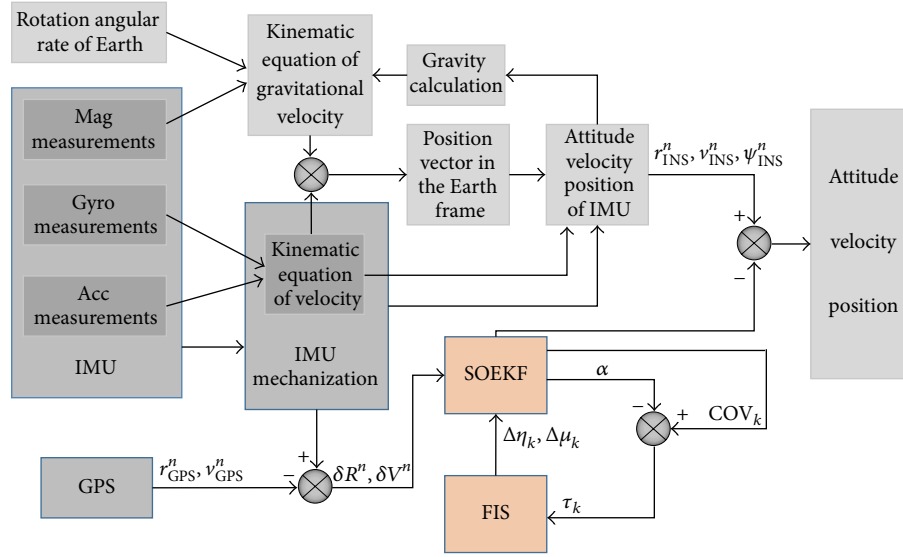


FIGURE 3: Proposed hybrid FIS-SOEKF model in navigation system.

correlation time. As it has been mentioned before, using the identification algorithms (i.e., YW, Burge's, and MCOV algorithms) to estimate the ARP's coefficients of the combined IGMP-ARP model is the goal of this section. Furthermore, in order to compare the combined IGMP-ARP model with classical IGMP model, first the IGMP parameters are experimentally estimated by ACF; then the parameters are obtained by ARP using different identification algorithms.

Furthermore, Wavelet Denoising Technique (WDT) can be combined with the ACF (as the experimental method to estimate the classical IGMP parameters) or with proposed combined IGMP-ARP (as an alternative method to estimate the parameters of IGMP) to investigate the stochastic error of inertial sensors. After applying the technique, the coefficients of IGMP obtained by ARP, or ACF, were determined from the enduring noises. These combinations are augmented in GPS/INS integration system to improve the navigational solution and their results are presented in Section 4.

**3.2. Proposed Hybrid FIS-SOEKF Model for GPS/INS Integration.** Two different approaches of adaptive Kalman filtering, namely, Innovation Adaptive Estimation (IAE) and Multiple Model Adaptive Estimation (MMAE), are considered by several research groups [32, 33]. These two approaches are based on Covariance Matching Estimation Technique (COMET). This study adopted the IAE concept in the fuzzy part of the proposed model.

The dynamic characteristics of vehicle motion in body frame and the navigation frame form the basis for the SOEKF process. The FIS can be exploited to increase the accuracy and the robustness of the SOEKF and to prevent its divergence in the tuning phase of SOEKF. Hence, FIS was used as a structure for identifying the dynamic variations and for implementing the real-time tuning of the nonlinear error model. It can provide a good estimation in maintaining the accuracy and

the tracking-capability of the system. Figure 3 depicts how the proposed hybrid FIS-SOEKF model performs as the ubiquitous navigation system.

Fuzzy Inference System (FIS) is a rule-based expert method that can mimic human thinking and understand linguistic concepts, rather than the typical logic systems [34]. The advantage of the FIS is realized when the algorithm of the estimation states becomes unstable because of the high complexity of the system. FIS are also used for the knowledge induction process, because they can serve as estimators for general purpose [35].

FIS architecture performs three types of operations: fuzzification, fuzzy inference, and defuzzification. Fuzzification converts the crisp input values into fuzzy values; fuzzy inference maps the given inputs into an output, and defuzzification converts the fuzzy operation into the new crisp values. The FIS can convert the inaccurate data to normalized fuzzy crisps, which are represented by the ranges of possible values, Membership Functions (MFs), and the confidence-rate of the inputs. In addition, the FIS are capable of choosing an optimal MF under certain specific criteria, applicable to a specific application. The deterministic output of FIS and its performance depend on the effective fuzzy rules, the considered defuzzification process, and the reliability of the MF values.

The proposed FIS model is based on the innovation process of the covariance matrix as the input of the FIS as well as the difference between the actual covariance matrix and the theoretical covariance matrix. Figure 4 shows the proposed FIS overview, which was used in this study. The theoretical covariance matrix, based on the innovation process, was computed partly in SOEKF by (4). The actual covariance matrix, according to [36], presented is proposed by

$$\alpha = \frac{1}{D} \sum_{i=k-D+1}^k v_i v_i^T, \quad (18)$$

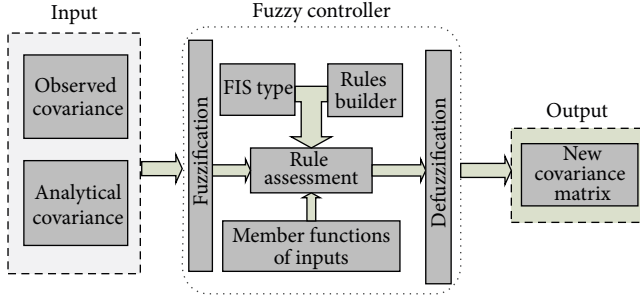


FIGURE 4: Proposed FIS part for hybrid FIS-SOEFK in navigation system.

where  $D$  is the window size (it is designated by moving window techniques and experimentally chosen as  $D = 20$ ) and  $v_i$  is  $[v_1 \ v_2 \ \dots \ v_m]^T$ . So, the difference is presented by

$$\begin{aligned} \tau = \text{COV}_k - \alpha &= \frac{1}{D} \\ &\cdot \sum_{i=k-D+1}^k \left\{ H_x(x_k^-, k) P_k^- H_x^T(x_k^-, k) \right. \\ &+ \frac{1}{2} \sum_{i,i'} e_i e_{i'}^T \text{tr} \left\{ H_{xx}^{(i)}(x_k^-, k) P_k^- H_{xx}^{(i')} x_k^-, k P_k \right\} + \mu_k \\ &\left. - v_k v_k^T \right\}. \end{aligned} \quad (19)$$

In fact,  $\tau$  can display the Degree of Incompatibility (DOI) between the actual and the theoretical covariance matrices. When  $\tau$  is near zero, it means that these two values nearly match and the absolute value of the difference can be negligible. However, if  $\tau$  is smaller or greater than zero, it means that the theoretical value ( $\text{COV}_k$ ) is greater or smaller than the actual value ( $\alpha$ ). To correct this difference, the diagonal element of  $\mu_k$  in (4) should be adjusted relying on the DOI. The proposed rules of assessment, according to the difference between the actual and the theoretical covariance matrices, are described as three scenarios of FMs:

- (1) If  $\tau$  is greater than 0, then  $\mu_k$  will decrease due to  $\delta\mu_k$ .
- (2) If  $\tau$  is less than 0, then  $\mu_k$  will increase due to  $\delta\mu_k$ .
- (3) If  $\tau \cong 0$ , then  $\mu_k$  will remain unchanged.

Consider  $\delta\mu_k = \mu_k - \mu_{k-1}$ . The related FMs are shown in Figure 5(a), wherein “D,” “B,” and “I” denote “Decrease,” “Balance,” and “Increase,” respectively. In addition, (2) and (5) show that if  $\mu_k$  is perfectly observed, variation in  $\eta_k$  can make changes in  $\text{COV}_k$ , directly. So, with the observation of the incompatibility between the actual and the theoretical covariance matrices, augmentation, or diminishment becomes essential for  $\eta_k$ . The proposed rules of assessment for this purpose are described as two MFs of FIS:

- (1) If  $\tau_k - \tau_{k-1} = 0$ , then  $\eta_k$  will remain unchanged.
- (2) If  $\tau_k - \tau_{k-1} \neq 0$ , then  $\eta_k$  will change due to  $\delta\eta_k$ .

TABLE 1: Technical specification of the angular rate and the acceleration sensors in micro-iBB.

Accelerometer		Gyroscope	
Data rate	200 Hz	Data rate	200 Hz
Temperature range	-40~+85°C	Temperature range	-40~+85°C
Input range	±2 g	Input range	±250°/sec
Linear sensitivity	2 mg/LSB	Sensitivity	m°/sec/digit
Acceleration noise density	220 μg/√Hz	Rate noise density	0.03°/sec/√Hz
		Nonlinearity	0.2%/sec

Consider  $\delta\eta_k = \eta_k - \eta_{k-1}$ . The related FMs are shown in Figure 5(b) wherein “LZ,” “Z,” and “GZ” denote “lower than zero,” “zero,” and “greater than zero,” respectively.

#### 4. Experimental Analysis, Results, and Discussion

The static raw data for analysis of the stochastic error was obtained from the wireless Micro-intelligent Black Box (Micro-iBB), which was designed and assembled by the VTADS team of the LASSENA Lab in the ETS. Micro-iBB consists of a triad of accelerometers, gyroscopes, magnetometers, and a temperature sensor. The serial numbers of the accelerometer, the gyroscope, and the demonstration board are LSM303DLHC, L3GD20, and STEVAL-MKI119V1, respectively. The selected aiding devices in Micro-iBB consist of a GNSS receiver (u-blox 7). Table 1 and Figure 6 present, respectively, the details of the Micro-iBB and its technical specification, which were used in this paper.

**4.1. Stochastic Error Modeling Technique.** This section analyzes the stochastic error to determine the effect of random errors on gyroscopes and accelerometers of the Micro-iBB. First, the ACFs were considered after recording the raw data. WDT was applied before data processing to weaken high frequency noises and remove preliminary biases in the sensors. By using WDT, uncorrelated and colored noises in the signal could be reduced. Figure 7 depicts the effect of different LODs in eliminating the system’s noise. Then, the related parameters of ACF for IGMP, namely,  $\sigma_{wk}^2$  and  $\beta$ , should be extracted. Figure 8(a) shows the ACF for accelerometers after using WDT with six LODs. This figure confirms the existence of residual noise along  $y$ -axis and  $z$ -axis of the accelerometers, even after applying the WDT. This noise is the uncorrelated term of the noise, which cannot be attenuated by the ACF in IGMP. The ACF of the  $x$ -axis of the accelerometer implies that the  $x$ -axis is more correlated than are the other axes.

Figure 8(b) shows the ACF of gyroscopes after using WDT with 6 LODs. This figure shows that although the  $y$ -axis and  $z$ -axis gyroscopes were influenced principally by HF and white noises, the  $x$ -axis of the gyroscope shows more correlated components than the other axes do. The comparison between Figures 1 and 8 clearly shows that

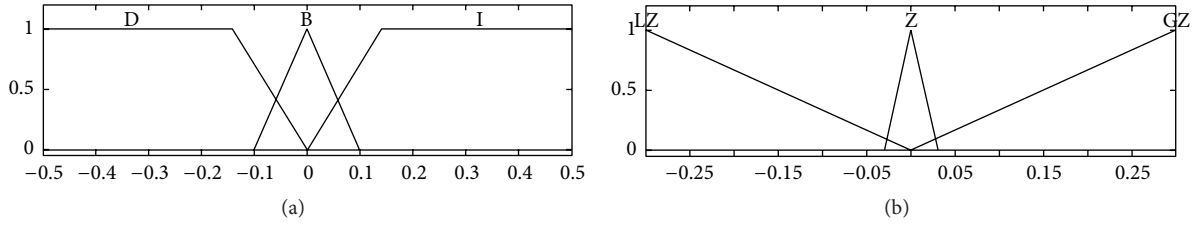


FIGURE 5: Membership Functions (MFs) for (a)  $\delta\mu_k$  and (b)  $\delta\eta_k$ .



FIGURE 6: Wireless Micro-intelligent Black Box (Micro-iBB).

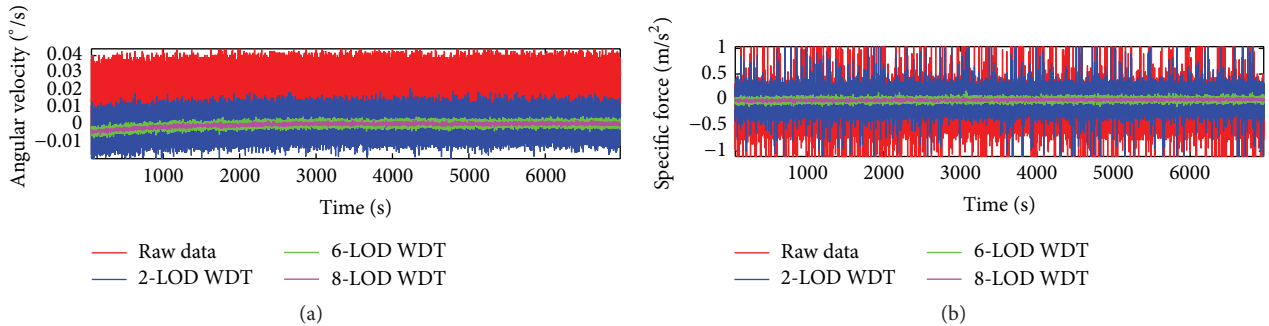


FIGURE 7: WDT with different LODs for (a)  $x$ -axis of accelerometers and (b)  $y$ -axis of gyroscopes, in Micro-iBB, in stationary situation.

the ACF cannot model the low-cost MEMS IMUs' errors with IGMP perfectly. Therefore, for this study, it was performed to model IGMP by utilizing ARP's parameters as an alternative solution to overcome this problem in the analysis of stochastic errors. The experimental results of ACF for all sensors are summarized in Table 2 under "ACF-based" column. Following this, MCOV, YW, and Burg's algorithms have also been applied to the denoised measurements (with different levels of decomposition) in order to estimate the parameters of combined IGMP-ARP. Results for these algorithms also are summarized in Table 2 under "YW-ARP-based," "MCOV-ARP-based," and "BURG's-ARP-based" columns for 6 levels of decomposition. These results present a considerable difference between the parameters obtained with each of the four identifications methods.

**4.2. GPS/INS Integration.** To evaluate the performance of the proposed models of GPS/INS integration, their results are compared with those of the conventional methods of GPS/INS integration. For demonstration, the loosely coupled GPS/INS integration was utilized in a three-dimensional navigation system. In the loosely coupled GPS/INS integration, position and velocity observed by GPS are the auxiliary measurements. So, in the SOEKF measurement model can be as follows:

$$\delta z = H\delta\bar{x} + \eta, \quad (20)$$

where  $H$  is  $\begin{bmatrix} H_R & 0_{3 \times 3} & 0_{3 \times 2} \\ 0_{3 \times 3} & H_R & 0_{3 \times 2} \end{bmatrix}$  and  $H_R = I_{3 \times 3}$ . Measurement noise vector  $\eta$  is  $[\eta_R \ \eta_V]^T$ , denoting the position and velocity noise. Vector  $\eta$  is defined by measurement noise model  $R$  in



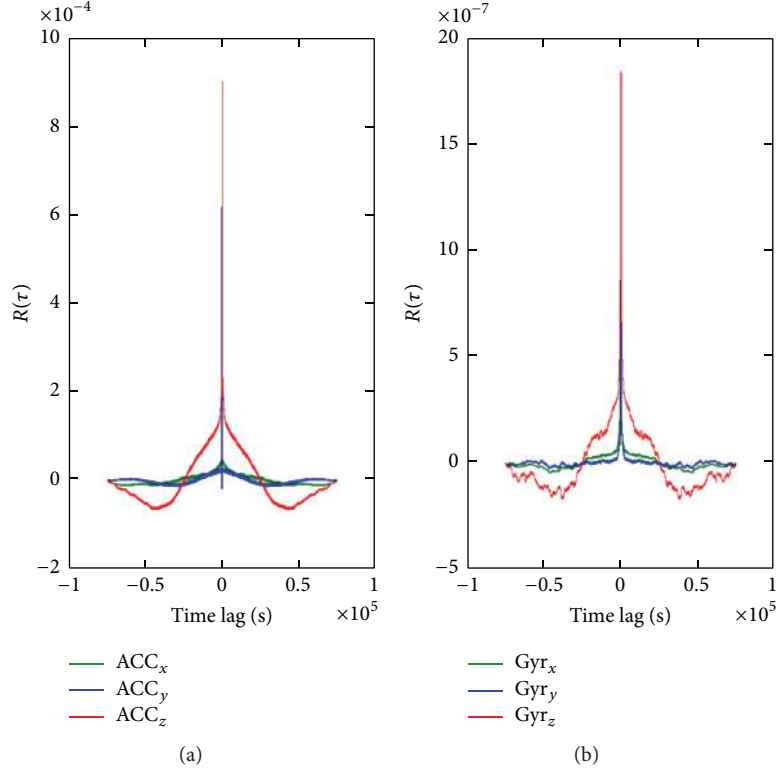


FIGURE 8: ACF of 1GMP for (a) accelerometers and (b) gyroscopes, in Micro-iBB after employing WDT with 6 LODs.

TABLE 2: The parameters needed to model 1GMP with different methods for ARP after 6 LODs of WTD.

Models	ACF-based		YW-ARP-based		MCOV-ARP-based		BURG's-ARP-based	
	$\sigma_{wk}^2$	$\beta$	$\sigma_{wk}^2$	$\beta$	$\sigma_{wk}^2$	$\beta$	$\sigma_{wk}^2$	$\beta$
Acc <sub>x</sub>	$3.2 \times 10^{-12}$	1/2600	$3.4 \times 10^{-10}$	1/380	$1.4 \times 10^{-11}$	1/740	$1.6 \times 10^{-11}$	1/1100
Acc <sub>y</sub>	$2.9 \times 10^{-11}$	1/2300	$3.8 \times 10^{-9}$	1/740	$1.8 \times 10^{-11}$	1/1100	$3.1 \times 10^{-11}$	1/1500
Acc <sub>z</sub>	$7.1 \times 10^{-12}$	1/1100	$5.4 \times 10^{-10}$	1/320	$4.6 \times 10^{-11}$	1/630	$5.1 \times 10^{-11}$	1/900
Gyr <sub>x</sub>	$2.5 \times 10^{-12}$	1/1700	$4.1 \times 10^{-10}$	1/60	$3.9 \times 10^{-11}$	1/520	$6.2 \times 10^{-11}$	1/1600
Gyr <sub>y</sub>	$1.8 \times 10^{-12}$	1/800	$6.7 \times 10^{-10}$	1/150	$2.5 \times 10^{-11}$	1/330	$4.1 \times 10^{-11}$	1/500
Gyr <sub>z</sub>	$3.7 \times 10^{-12}$	1/1500	$4.3 \times 10^{-10}$	1/90	$2.1 \times 10^{-11}$	1/570	$3.7 \times 10^{-11}$	1/1200

SOEKF, where  $R = \text{diag} [\delta_R^2 \delta_R^2 \delta_R^2 \delta_V^2 \delta_V^2 \delta_V^2]$  is modeled according to the GPS position and velocity uncertainty with zero mean and covariance matrix. The error states vector, relating to the navigation system of this study, is as follows:

$$\delta \bar{x} = [\delta \bar{R} \quad \delta \bar{V} \quad \delta \bar{\psi} \quad \delta \bar{b}_g \quad \delta \bar{b}_a]^T, \quad (21)$$

where  $\delta \bar{R}$  and  $\delta \bar{V}$  are, respectively,  $[\delta R_N \quad \delta R_E \quad \delta R_U]$  and  $[\delta V_N \quad \delta V_E \quad \delta V_U]$ , denoting position and velocity residual errors in East North Up (ENU) frame;  $\delta \bar{\psi}$  is  $[\delta \psi_N \quad \delta \psi_E \quad \delta \psi_U]$  and is the attitude error.  $\delta \bar{b}_g$  and  $\delta \bar{b}_a$  are, respectively,  $[\delta b_{g_x} \quad \delta b_{g_y} \quad \delta b_{g_z}]$  and  $[\delta b_{a_x} \quad \delta b_{a_y} \quad \delta b_{a_z}]$ , denoting the stochastic error states of accelerometers and gyroscopes along the three axes. In fact,  $\delta \bar{b}_g$  and  $\delta \bar{b}_a$  are included in the state vector of error propagation model to dynamically estimate the six stochastic error states. From the definition of 1GMP

in (10), the dynamic equations related to stochastic error states of accelerometers and gyroscopes can be shown by

$$\begin{bmatrix} \delta \dot{b}_g \\ \delta \dot{b}_a \end{bmatrix} = \begin{bmatrix} \beta_g & 0 \\ 0 & \beta_a \end{bmatrix} \begin{bmatrix} \delta \bar{b}_g \\ \delta \bar{b}_a \end{bmatrix} + \begin{bmatrix} w_g \\ w_a \end{bmatrix}. \quad (22)$$

Table 2 presents the 1GMP's parameters which are estimated by ACF and the combined 1GMP-ARP (using different algorithms) for 6 LODs of WTD. So, the  $\beta_g$ ,  $\beta_a$ ,  $w_g$ , and  $w_a$  in (21) can be initialized by the values in Table 2 for 6 LODs of WTD.

The proposed land-navigation solution was implemented with an experimental setup for a road test. The tests were performed by Micro-iBB, whose specifications are detailed under Section 4.1. The results were evaluated against a reference solution provided by Novatel SPAN technology. It consists of Novatel receiver and Honeywell tactical-grad IMU

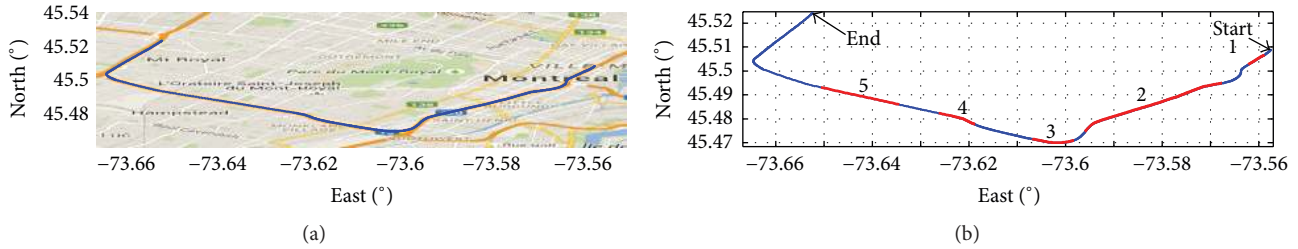


FIGURE 9: The freeway trajectory showing the five outages: (a) on google map and (b) on Matlab.

to validate the proposed method and to assess the overall performance during the GPS outages.

The raw data of the route-test was gathered from different sensors of Micro-iBB. The selected trajectories satisfy the overall quality and reliability requirements of the proposed models of this study in real environments of various conditions. The first trajectory was figured out in an urban freeway which allowed the authors to drive at high speed. The second trajectory was in downtown area that contains numerous prominent skyscrapers. The test along this trajectory was performed at slow speed with frequent stops because of high traffic and crowded road intersections.

The goal is to investigate the efficiency of the proposed hybrid FIS-SOEKF using different LODs of WDT and using various algorithms to estimate ARP's coefficients for IGMP. The WDTs considered for this purpose are 2 LODs, 6 LODs, and 8 LODs and the algorithms are MCOV, YW, and Burg's algorithm. The proposed combinations are compared with traditional SOEKF and two hybrid FIS-SOEKFs, which used ACF to estimate the IGMP coefficient with different LODs of WDT. All the hybrid FIS-SOEKF solutions followed the idea of updating stochastic error states to the gyroscope and accelerometers measurements. RMSEs were estimated in all navigational solutions with Novatel SPAN as the reference solution.

**4.2.1. First Scenario: Freeway.** The first route-test trajectory selected for this study starts from freeway #5 near Viger East Avenue (45.509023, -73.557511) and ends at freeway #71 near Lebeau Avenue (45.524299, -73.652472) in Montreal, QC, Canada, by boulevard Ville-Marie/highway #720 West and highway #15 North (see Figure 9). This trajectory was done for nearly 11 min of uninterrupted car navigation over a distance of 14.4 km. The freeway trajectory was chosen with five natural GPS outages to examine the system's performance during short and long outages that exist in urban canyons. Figure 9(a) depicts the route-test with the reference solution on google map. Figure 9(b) presents the position of the GPS outages on Matlab with red lines, along the selected trajectory.

Figure 10 presents the number of available satellites and the time-duration of each GPS outage. The first GPS outage in tunnel area occurred for 30 sec with less than number of 7 available satellites. There was no satellite for about two-thirds of the duration of this outage (see Figure 10(a)). The second and third outages occurred along the two skyways for 180 sec and 60 sec durations (see Figures 10(b)-10(c)). Figures

10(d)-10(e) present the last two outages in urban canyon area for durations of 50 and 30 sec. Generally, higher moving speed increases horizontal positioning errors. Therefore, this scenario of high speed driving with several outages can test the validity and robustness of the proposed models.

Figure 11 presents the root mean square and the maximum errors in horizontal positioning during the five GPS outages in the first scenario for the twelve compared solutions. The advantage of using the proposed method with 6 LODs for updating stochastic error states to gyroscope and accelerometer measurements can be seen by comparing it with the traditional SOEKF and hybrid FIS-SOEKFs, which are used in ARP or ACF to estimate the IGMP coefficient, utilizing different LODs of WDT. Figure 11 illustrates the results obtained by (i) the traditional SOEKF without updating stochastic error states, shown as SOEKF, and (ii) those obtained by the proposed hybrid FIS-SOEKF, using ACF-based IGMP, after 2-LOD denoising, shown as "FS(ACF2)," and after 6-LOD denoising, shown as "FS(ACF6)." The rest of the solutions used the proposed hybrid FIS-SOEKF and are shown as "FS" in this figure. (iii) "MCOV-ARP," "YW-ARP," and "BURG's-ARP" represent the solutions that modeled IGMP by using ARP's coefficients under "modified-covariance," "Yule-Walker," and "Burg's" algorithms, respectively. The values, which follow each solution, denote the specific LOD of WDT that was used in that solution.

From the foregoing data, it can be seen that the proposed hybrid FIS-SOEKF, which used ACF-based IGMP after 6-LOD denoising, performed significantly better than did the traditional SOEKF without updating stochastic error states. This is because the proposed hybrid FIS-SOEKF can deal with the nonlinearity of systems and models; however, SOEKF exploits second-order linearized models to estimate the state of systems. The results also show that "BURG's-ARP" outperformed "SOEKF" and also the proposed hybrid FIS-SOEKF that used ACF-based IGMP after denoising.

Furthermore, in terms of the ARP-based IGMP after 6-LOD denoising, "BURG's-ARP6" shows a major improvement in positioning accuracy as compared with the performance of "YW-ARP6" and "MCOV-ARP6." This is because Burg's algorithm provides the highest accuracy when applied to low-cost MEMS-based INS as compared to the other algorithms that determine the ARP's coefficients ideally. During the second outage of 180 sec duration, it can be seen that the performance of all solutions degraded considerably, because at least four satellites are needed in loosely coupled

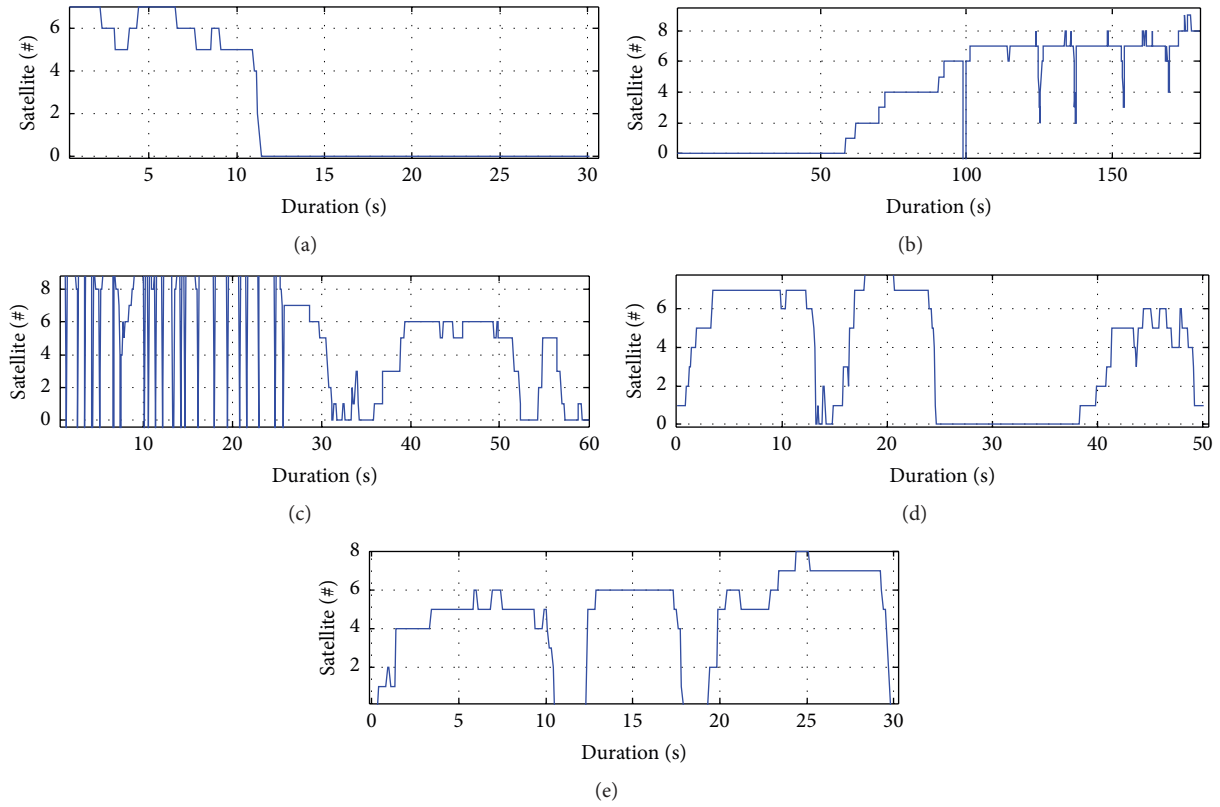


FIGURE 10: Available satellites in each outage for freeway trajectory: (a) outage #1, (b) outage #2, (c) outage #3, (d) outage #4, and (e) outage #5.

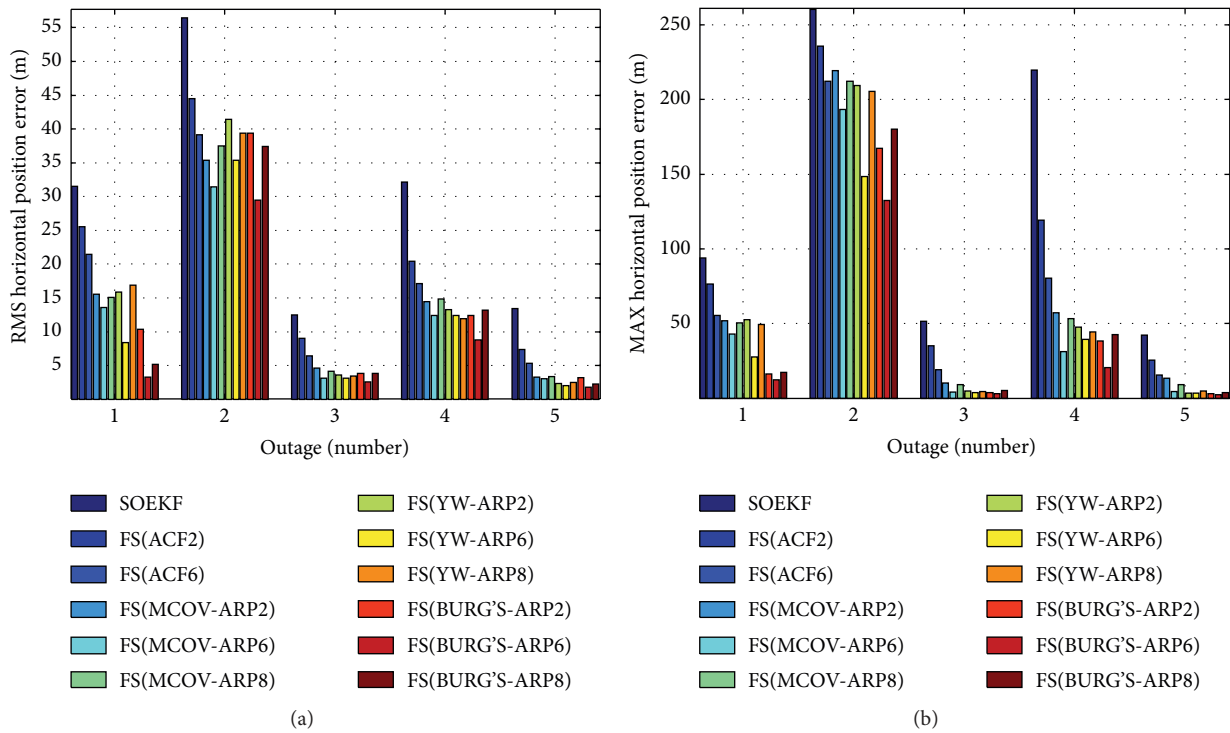


FIGURE 11: (a) Root mean square error and (b) maximum errors, in horizontal positioning during five GPS outages in the first scenario (freeway).

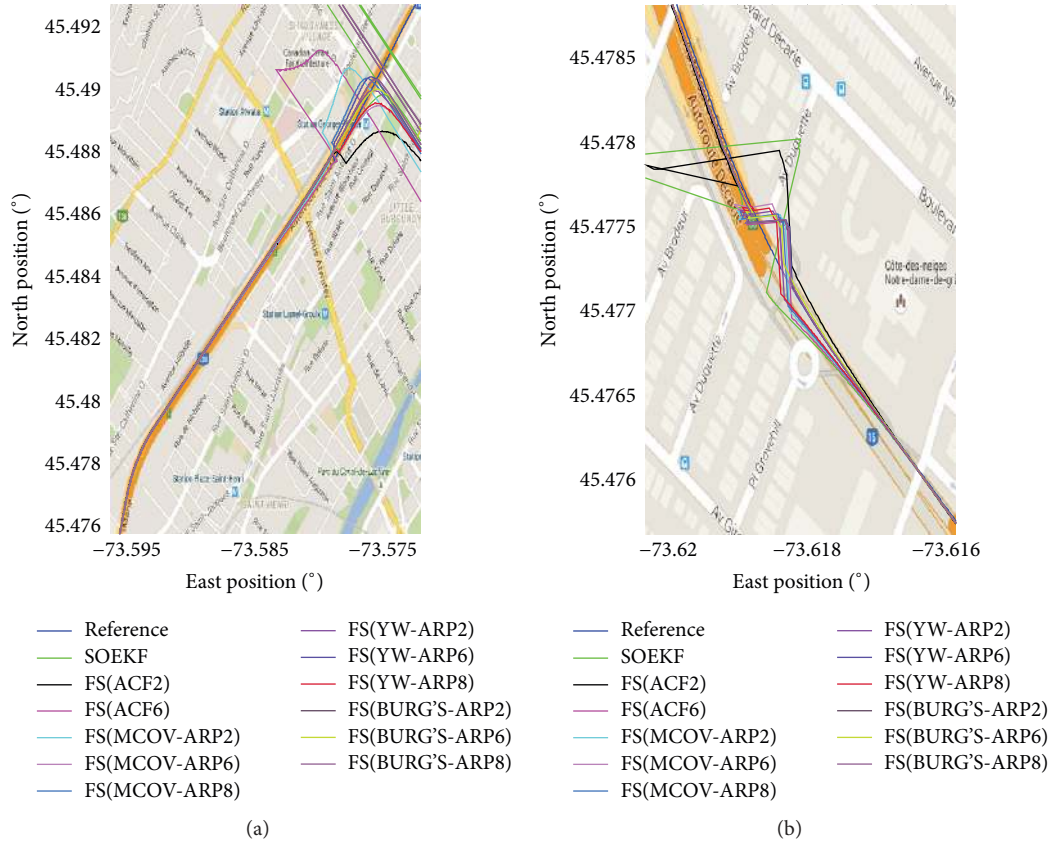


FIGURE 12: Different navigation solutions for the freeway trajectory: (a) outage #2 and (b) outage #4.

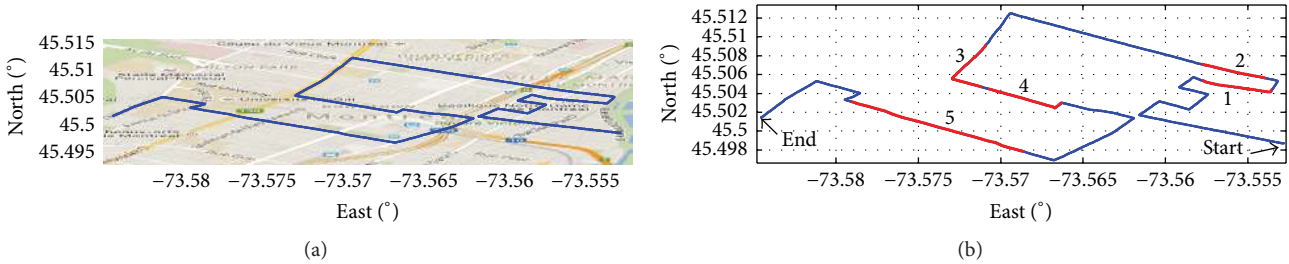


FIGURE 13: Second (downtown) trajectory showing the five outages: (a) on google map and (b) on Matlab.

GPS/INS integration. Against this requirement, the number of satellites available was less than four for more than half of the outage duration, besides the duration itself being quite long. In addition, using the low-cost MEMS-based INS worsened this situation. So, the second outage gave the worst result, with the maximum horizontal error being 630 m and mean horizontal error 187 m; these cannot be shown in the figure as the values are high.

Figure 12 presents two sections of the freeway trajectory during GPS outages #2 and #4. This figure shows the reference and all the navigation solutions considered in this paper. These results confirm that the performance of the proposed hybrid FIS-SOEKF, used with ARP-based IGMP after 6-LOD denoising, is acceptable as a new navigational solution

in freeways where the duration of GPS outages can be a maximum of 60 sec.

4.2.2. *Second Scenario: Downtown.* The second route-test trajectory selected starts from McGill Street near La Commune Ouest Avenue (45.498718, -73.552831) and ends up at Pins Ouest Avenue (45.501466, -73.584548) in Montreal, QC, Canada, by Boulevard St-Laurent/Shebrooke Ouest Street and Peel Street (see Figure 13). Testing along this trajectory was carried out through medium and high traffic volumes for nearly 50 min of car navigation covering a distance of 10.5 km. This downtown trajectory, which runs through skyscrapers, was chosen because of its five natural GPS outages to examine the system's performance during short and long outages.



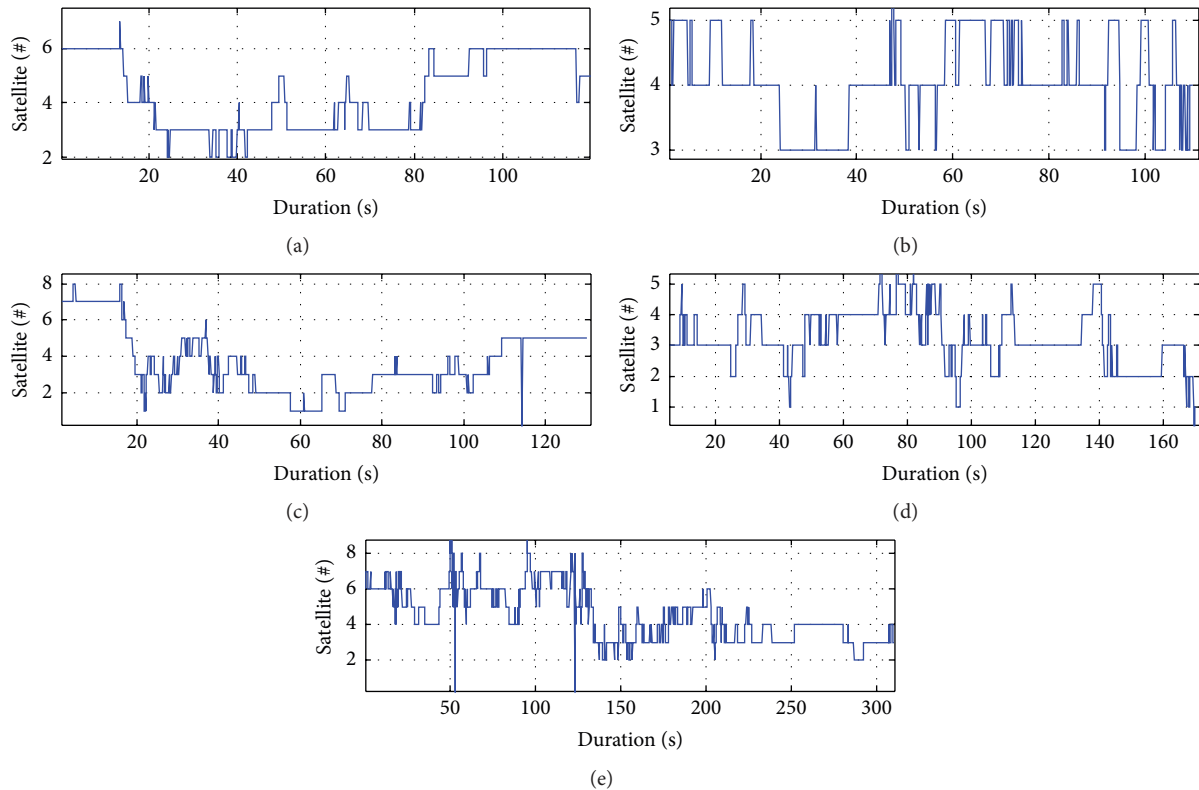


FIGURE 14: Available number of satellites during each outage for downtown trajectory: (a) outage #1, (b) outage #2, (c) outage #3, (d) outage #4, and (e) outage #5.

Figure 13(a) depicts route-test with the reference solution on google map. Figure 13(b) presents the details of the position of the GPS outages on Matlab with red lines, along the selected trajectory.

Figure 14 shows the number of available satellites and the time-duration of each GPS outage for downtown trajectory of Montreal. To examine the proposed navigation solution during longer GPS outages, the near outages were clubbed into bigger outages. The number of the bigger outages in this scenario thus became 5. Figure 15 shows the RMSE and the maximum error in horizontal positioning during the five GPS outages for the twelve compared solutions. The results of this scenario confirm the accuracy obtained in the results of the previous scenario.

Figure 16 illustrates the results obtained for outages #2 and #4, by (i) the traditional SOEKF without updating stochastic error states, shown as “SOEKF”, and (ii) those obtained by the proposed hybrid FIS-SOEKF using ACF-based 1GMP after 2-LOD denoising, shown as “FS(ACF2),” and after 6-LOD denoising, shown as “FS(ACF6).” (iii) The rest of the solutions used the proposed hybrid FIS-SOEKF which are shown as “FS.” “MCOV-ARP,” “YW-ARP,” and “BURG’s-ARP” represent the solutions that modeled 1GMP by using ARP’s coefficients under “modified-covariance,” “Yule-Walker,” and “Burg’s” algorithms, respectively. The values that follow each solution denote the specific LOD of WTD that was used in that solution.

From the data presented, it can be seen that the proposed hybrid FIS-SOEKF, which used ACF-based 1GMP after 2-LOD and 6-LOD denoising, “FS(ACF2)” and “FS(ACF6),” performed significantly better than did the traditional SOEKF without updating stochastic error states. The results also show that “FS(BURG’s-ARP),” among all the “SF (ARP)” navigation solutions, outperformed “SOEKF,” “FS(ACF2),” and “FS(ACF6).” Furthermore, in terms of the ARP-based 1GMP after 6-LOD denoising, “FS(BURG’s-ARP6)” shows a major improvement in positioning accuracy in the downtown scenario, as compared with the accuracy obtained by “FS(YW-ARP6)” and “FS(MCOV-ARP6).” This is because Burg’s algorithm provides the highest accuracy when applied to low-cost MEMS-based INS, as compared to the other algorithms that determine the ARP’s coefficients perfectly.

As regards the number of satellites and the duration of each GPS outage, it can be seen that there are less than 4 satellites for two-thirds of the duration and less than 5 satellites during the remaining part of the duration for outages #2 and #4. However, RMSE in outage #4 is much more than that in outage #2, because the duration of outage #4 (180 sec) is longer than that of outage #2 (110 sec). The results also show that outage #5 presents, in spite of its longest duration (310 sec), lesser RMSE than that of outages #3 and #4. This is because 6–8 satellites existed for less than half of the duration of outage #4 and less than 4 satellites for three-quarters of the duration. Outage #2 shows the lowest error (2 m) because of its short outage duration.



## 5. Conclusions

In this paper, two novel auxiliary methods are proposed to improve the performance of ultralow-cost MEMS-based IMU in a vehicular navigation system. The proposed methods can cover two areas: modeling stochastic errors and performing GPS/INS integration. The proposed IGMP-ARP consists of a complete stochastic error modeling of the noise components in MEMS low-cost inertial sensors. This paper shows a big cooperation between IGMP, ARP, and WDT to characterize the noise components. Different levels of decomposition in denosing technique as well as various methods to identify the ARP parameters were considered to clarify the best one for stochastic error modeling in MEMS low-cost inertial sensors. Result presents that Burg's method, after applying the six levels of decomposition in denosing technique, performs much better than modified-covariance and Yule-Walker methods with different levels of decomposition. The second proposed method consists of an integration of SOEKFFIS to enhance the performance of low-cost GPS/INS integration for navigation data fusion. The FIS part is exploited for dynamic adjustment of the process noise covariance, by observing the innovation process, which is utilized in SOEKF-part to maintain further enhancement in the estimation of the accuracy. The results confirm that the proposed hybrid FIS-SOEKF can provide further improvement in the overall performance compared to SOEKF in harsh environment.

Future research work related to this study will focus on more complicated GPS/INS integration structures such as tightly and ultratightly coupled and noise modeling with higher order stochastic error to reduce the errors in the positing of the navigation system. In addition, GPS/INS integration will expand to GNSS/BDS/low-cost-INS integration to utilize the advantages of the multi-GNSS environment.

## Competing Interests

The authors declare that they have no competing interests.

## Acknowledgments

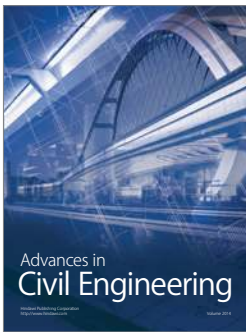
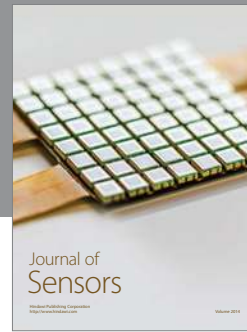
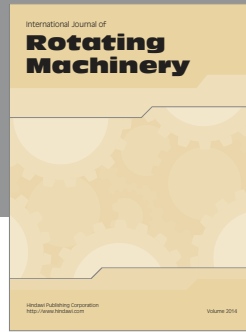
This research is part of the project entitled VTADS: Vehicle Tracking and Accident Diagnostic System. It is supported by the Natural Sciences and Engineering Research Council of Canada (NSERC) and École de Technologie Supérieure (LASSENA Lab), in collaboration with two industrial partners, namely, iMetrik Global Inc. and Future Electronics.

## References

- [1] J. W. Zellner, R. M. van Auken, D. P. Chiang, P. C. Broen, J. Kelly, and Y. Sugimoto, "Extension of the Honda-DRI 'Safety Impact Methodology' (SIM) for the NHTSA Advanced Crash Avoidance Technology (ACAT) program and application to a prototype advanced collision mitigation braking system," *SAE International Journal of Passenger Cars—Mechanical Systems*, vol. 2, no. 1, pp. 875–894, 2009.
- [2] T. Hai Ta, D. Minh Truong, T. Thanh Thi, H. Nguyen, T. Dinh Nguyen, and G. Belforte, "Multi-GNSS positioning campaign in South-East Asia," *Coordinates*, vol. 9, pp. 11–20, 2013.
- [3] D. M. Truong and T. H. Ta, "Development of real multi-GNSS positioning solutions and performance analyses," in *Proceedings of the International Conference on Advanced Technologies for Communications (ATC '13)*, pp. 158–163, Ho Chi Minh, Vietnam, October 2013.
- [4] K.-P. Schwarz and N. El-Sheimy, "Future positioning and navigation technologies," in *Study Performed under the Scientific Services Agreement with Batelle*, Columbus Division and Topographic Engineering Center, Fort Belvoir, VA, USA, 1999.
- [5] M. S. Grewal, L. R. Weill, and A. P. Andrews, *Global Positioning Systems, Inertial Navigation, and Integration*, John Wiley & Sons, New York, NY, USA, 2007.
- [6] J. Georgy, U. Iqbal, and A. Noureldin, "Quantitative comparison between kalman filter and particle filter for low cost INS/GPS integration," in *Proceedings of the 6th International Symposium on Mechatronics and its Applications (ISMA '09)*, pp. 1–7, Sharjah, United Arab Emirates, March 2009.
- [7] A. Oppenheim and R. Schaffer, *Discrete-Time Signal Processing: Pearson New International Edition*, Pearson Education, Upper Saddle River, NJ, USA, 2013.
- [8] A. Noureldin, T. B. Karamat, M. D. Eberts, and A. El-Shafie, "Performance enhancement of MEMS-based INS/GPS integration for low-cost navigation applications," *IEEE Transactions on Vehicular Technology*, vol. 58, no. 3, pp. 1077–1096, 2009.
- [9] T. B. Karamat, *Implementation of tightly coupled INS/GPS integration for land vehicle navigation [M.S. thesis]*, Electrical engineering, Royal Military College of Canada, 2009.
- [10] J. Pusa, *Strapdown inertial navigation system aiding with non-holonomic constraints using indirect Kalman filtering [M.S. thesis]*, Department of Mathematics, Tampere University of Technology, 2009.
- [11] Z. Shen, J. Georgy, M. J. Korenberg, and A. Noureldin, "Low cost two dimension navigation using an augmented Kalman filter/Fast Orthogonal Search module for the integration of reduced inertial sensor system and Global Positioning System," *Transportation Research Part C: Emerging Technologies*, vol. 19, no. 6, pp. 1111–1132, 2011.
- [12] L. Zhao, H. Qiu, and Y. Feng, "Study of robust  $H_\infty$  filtering application in loosely coupled INS/GPS system," *Mathematical Problems in Engineering*, vol. 2014, Article ID 904062, 10 pages, 2014.
- [13] P. Aggarwal, Z. Syed, and N. El-Sheimy, "Hybrid Extended Particle Filter (HEPF) for integrated civilian navigation system," in *Proceedings of the IEEE/ION Position, Location and Navigation Symposium (PLANS '08)*, pp. 984–992, Monterey, Calif, USA, May 2008.
- [14] J. Cheng, D. Chen, R. Landry Jr., L. Zhao, and D. Guan, "An adaptive unscented kalman filtering algorithm for MEMS/GPS integrated navigation systems," *Journal of Applied Mathematics*, vol. 2014, Article ID 451939, 8 pages, 2014.
- [15] K.-W. Chiang and Y.-W. Huang, "An intelligent navigator for seamless INS/GPS integrated land vehicle navigation applications," *Applied Soft Computing Journal*, vol. 8, no. 1, pp. 722–733, 2008.
- [16] A. Noureldin, A. El-Shafie, and M. R. Taha, "Optimizing neuro-fuzzy modules for data fusion of vehicular navigation systems using temporal cross-validation," *Engineering Applications of Artificial Intelligence*, vol. 20, no. 1, pp. 49–61, 2007.

- [17] L. Semeniuk and A. Noureldin, "Modeling of INS position and velocity errors using radial basis function neural networks for INS/GPS integration," in *Proceedings of the ION National Technical Meeting*, pp. 18–20, Monterey, Calif, USA, January 2006.
- [18] A. Noureldin, A. El-Shafie, and M. Bayoumi, "GPS/INS integration utilizing dynamic neural networks for vehicular navigation," *Information Fusion*, vol. 12, no. 1, pp. 48–57, 2011.
- [19] J. Škaloud, *Optimizing georeferencing of airborne survey systems by INS/DGPS [Ph.D. thesis]*, Department of Geomatics Engineering, Alberta, Canada, 1999.
- [20] Y. Bar-Shalom, X. R. Li, and T. Kirubarajan, *Estimation with Applications to Tracking and Navigation: Theory Algorithms and Software*, John Wiley & Sons, New York, NY, USA, 2004.
- [21] B. Sadeghi and B. Moshiri, "Second-order EKF and unscented Kalman filter fusion for tracking maneuvering targets," in *Proceedings of the IEEE International Conference on Information Reuse and Integration (IEEE IRI '07)*, pp. 514–519, IEEE, Las Vegas, Nev, USA, August 2007.
- [22] R. Ardito, C. Comi, A. Corigliano, and A. Frangi, "Solid damping in micro electro mechanical systems," *Meccanica*, vol. 43, no. 4, pp. 419–428, 2008.
- [23] A. Kumar and D. Chakraborty, "Effective properties of thermo-electro-mechanically coupled piezoelectric fiber reinforced composites," *Materials & Design*, vol. 30, no. 4, pp. 1216–1222, 2009.
- [24] M. Kleiber and T. D. Hien, *The Stochastic Finite Element Method: Basic Perturbation Technique and Computer Implementation*, Wiley-Interscience, 1992.
- [25] M. Kamiński and A. Corigliano, "Sensitivity, probabilistic and stochastic analysis of the thermo-piezoelectric phenomena in solids by the stochastic perturbation technique," *Meccanica*, vol. 47, no. 4, pp. 877–891, 2012.
- [26] M. El-Diasty and S. Pagiatakis, "A rigorous temperature-dependent stochastic modelling and testing for MEMS-based inertial sensor errors," *Sensors*, vol. 9, no. 11, pp. 8473–8489, 2009.
- [27] P. Lavoie, *Système de Navigation Hybride GPS/INS à Faible Coût pour la Navigation Robuste en Environnement Urbain*, M. Ing., Génie Électrique, École de Technologie Supérieure, Montreal, Canada, 2012.
- [28] S. Nassar, K.-P. Schwarz, N. El-Sheimy, and A. Noureldin, "Modeling inertial sensor errors using autoregressive (AR) models," *Navigation*, vol. 51, no. 4, pp. 259–268, 2004.
- [29] S. Nassar, K.-P. Schwarz, N. El-Sheimy, and A. Noureldin, "Modeling inertial sensor errors using autoregressive (AR) models," *Navigation, Journal of the Institute of Navigation*, vol. 51, no. 4, pp. 259–268, 2004.
- [30] C. H. Kang, S. Y. Kim, and C. G. Park, "Improvement of a low cost MEMS inertial-GPS integrated system using wavelet denoising techniques," *International Journal of Aeronautical and Space Sciences*, vol. 12, no. 4, pp. 371–378, 2011.
- [31] N. El-Sheimy, S. Nassar, and A. Noureldin, "Wavelet de-noising for IMU alignment," *IEEE Aerospace and Electronic Systems Magazine*, vol. 19, no. 10, pp. 32–39, 2004.
- [32] F. Jiancheng and Y. Sheng, "Study on innovation adaptive EKF for in-flight alignment of airborne POS," *IEEE Transactions on Instrumentation and Measurement*, vol. 60, no. 4, pp. 1378–1388, 2011.
- [33] J. Ma, S. Ni, W. Xie, and W. Dong, "An improved strong tracking multiple-model adaptive estimation: a fast diagnosis algorithm for aircraft actuator fault," *Transactions of the Institute of Measurement and Control*, 2015.
- [34] D. Bhatt, P. Aggarwal, V. Devabhaktuni, and P. Bhattacharya, "A new source difference artificial neural network for enhanced positioning accuracy," *Measurement Science and Technology*, vol. 23, no. 10, Article ID 105101, 2012.
- [35] L. M. Bergasa, J. Nuevo, M. A. Sotelo, R. Barea, and M. E. Lopez, "Real-time system for monitoring driver vigilance," *IEEE Transactions on Intelligent Transportation Systems*, vol. 7, no. 1, pp. 63–77, 2006.
- [36] R. Vershynin, "How close is the sample covariance matrix to the actual covariance matrix?" *Journal of Theoretical Probability*, vol. 25, no. 3, pp. 655–686, 2012.





**Hindawi**

Submit your manuscripts at  
<http://www.hindawi.com>

